

1 Spatial patterns of the Argentine hake *Merluccius hubbsi* and
2 oceanographic processes in a semi-enclosed Patagonian ecosystem.

3

4 **MATÍAS OCAMPO REINALDO** *^{1,2,3}, **RAÚL GONZÁLEZ**^{1,2}, **GABRIELA**
5 **WILLIAMS**⁴, **LORENA PÍA STORERO**^{1,2}, **MARÍA ALEJANDRA ROMERO**^{1,2},
6 **MAITE NARVARTE**^{1,2} **AND DOMINGO ANTONIO GAGLIARDINI**^{4,5}

7

8 ¹ Instituto de Biología Marina y Pesquera “Almirante Storni” (IBMPAS)/Escuela
9 Superior de Ciencias Marinas (ESCiMar), Universidad Nacional del Comahue, San
10 Antonio Oeste, Argentina.

11 ² Consejo Nacional de Investigaciones Científicas y Técnicas (CONICET), Ciudad
12 autónoma de Buenos Aires, Argentina.

13 ³ Leibniz Centre for Tropical Marine Ecology, Bremen, Germany

14 ⁴ Centro Nacional Patagónico (CENPAT, CONICET), Puerto Madryn, Argentina.

15 ⁵ Instituto de Astronomía y Física del Espacio (IAFE, CONICET), Ciudad autónoma de
16 Buenos Aires, Argentina

17

18 *Corresponding author: M. Ocampo Reinaldo. E-mail addresses: matiocre@gmail.com,
19 matiocre@ibmpas.org, matiocre@zmt-bremen.de. Tel: +54 (2920) 430764. Fax: +54
20 (2920) 421002. Postal address: Instituto de Biología Marina y Pesquera “Almirante
21 Storni”. Güemes 1030, (R8520CXV) San Antonio Oeste, Argentina.

22

23 Running title: Spatial patterns of Argentine hake.

24

25 Abstract

26 Time-series of fishing position, landings, satellite-derived sea surface temperature and
27 chlorophyll *a* concentrations were used to relate the spatial-temporal distribution of the
28 Argentine hake *Merluccius hubbsi* with seasonal oceanographic processes in San Matías
29 Gulf. Also, the seasonal effect of fishing on the hake population structure was analysed.
30 During summer the fleet was concentrated over the area of the frontal system, obtaining
31 the best catch-per-unit-effort (CPUE) of hake in relatively deep waters. In autumn, the
32 dispersion of the fleet due to a reduction in CPUE coincided with the dissipation of the
33 front, suggesting that the distribution and shoaling of the Argentine hake is associated
34 with seasonal thermal structures. In spring, the thermal structure of the waters and the
35 Chlorophyll *a* blooms seem to modulate the timing of spawning of hake, which occurs
36 mainly in October-November. In addition, the fleet captured a higher proportion of
37 females in the gonadal recovery stage during warm months (November to April). While
38 winter catches (May to October) consisted mainly of males, the intense summer fishing
39 may result in a high impact on the female population. This information is relevant to
40 design of spatial management tools intended to provide biological sustainability to the
41 hake fishery.

42

43 Keywords

44 Natural resources distribution, tidal front, trawl fishery, satellite-derived data,
45 sustainable management.

46

47 Introduction

48 The physical properties of the oceans influence biological processes at all spatial and
49 temporal scales (Mann 1992). Among the different physical variables that affect the
50 distribution of marine organisms, the sea temperature is considered important, because
51 many species are associated with thermal structures and specific thermal conditions
52 (Perrota *et al.* 2001; Spinelli *et al.* 2012). Various species show high densities next to
53 oceanic fronts (Reddy *et al.* 1995; Sabatini & Martos 2002), because these structures
54 play a key role in ecological processes by allowing for an exceptionally high primary
55 production, offering adequate feeding and/or reproductive habitats for nektonic species
56 (fishes and squids) and acting as retention areas for larvae (Acha *et al.* 2004; Houde
57 2009; Spinelli *et al.* 2012). Similarly, areas with high chlorophyll-*a* (Chl *a*)
58 concentrations, which indicate high phytoplankton biomass (Morel & André 1991; Huot
59 *et al.* 2007) are related to limiting concentrations of nutrients (Aminot *et al.* 1998; Herut
60 *et al.* 2007), show abundant fish and crustacean larvae (Wehrtmann 1994; Friedland *et*
61 *al.* 1996) and high concentration of birds (Ballance *et al.* 1997) and marine mammals
62 (Jaquet *et al.* 1996). In this respect, studying the areas with oceanic fronts and/or high
63 Chl *a* concentrations may also be relevant to design measures for fisheries management
64 and conservation.

65 On the Argentine Continental Shelf (ACS), frontal areas provide better foraging
66 opportunities than non-frontal areas for a broad range of marine organisms (Alemany *et*
67 *al.* 2009). Indeed, the oceanographic fronts are key marine structures in which to
68 understand feeding and reproduction strategies, as well as migration patterns of local
69 populations (Acha *et al.* 2004). Also, the thermal structure of the sea has been
70 considered as an important variable in biological and fisheries studies, mainly in the
71 prediction of recruitment, larval survival, spawning areas and catches as well as in the

72 study of spatial and temporal changes in abundance of commercial species (Stuart *et al.*
73 2011).

74 Considering that the fact that changes in sea surface temperature (SST) could be
75 used as an indicator of the structuring of water masses (i.e. thermal fronts) and also a
76 relevant factor in the distribution and concentration of nutrients and phytoplankton (and
77 consequently in the distribution and abundance of biological resources), integrated
78 satellite-derived information of the SST and Chl *a* concentrations could be useful for
79 analysing the relationships between distribution, abundance and catches of species of
80 ecological and/or fisheries importance (Laurs *et al.* 1984). In pelagic fisheries, this
81 approach has been widely used in scientific studies and commercial applications (e.g.
82 Polovina *et al.* 2001; Platt *et al.* 2007; Saitoh *et al.* 2011; Druon *et al.* 2011). Moreover,
83 fish species that integrate pelagic-demersal communities and develop most of their life
84 cycles interacting with the intermediate and upper layers of the ocean, are good
85 candidates for this type of study (Laurs *et al.* 1984). In the ACS, Wang *et al.* (2007)
86 studied the influence of thermal features on the distribution of *Merluccius hubbsi*
87 Marini, 1933 at the Patagonian shelf edge and found that hake have a positive
88 association with thermal oceanic features.

89 Within San Matías Gulf (SMG, Patagonia, Argentina), many fishery species that
90 play an important role in food webs (e.g. short-finned squid *Illex argentine*
91 Castellanos, 1960) show dramatic interannual abundance variations for unclear reasons
92 (Romero *et al.* 2007). Other species (e.g. *M. hubbsi*, the silver warehou *Seriolella*
93 *porosa* Guichenot, 1848 and the Patagonian hoki *Macruronus magellanicus* Lönnberg,
94 1907) show seasonal variations apparently related to cyclical oceanographic processes
95 (Ocampo Reinaldo 2010). Within this ecosystem, the fishing activity is performed
96 mainly by industrial bottom trawlers and historically the most important fishery

97 resource has been the Argentine hake (up to 80% of the annual landings) followed by
98 the silver warehou in recent years (Romero *et al.*, 2010). The Argentine hake has
99 demersal-pelagic habits, is an active predator that performs daily vertical migrations to
100 feed in the upper layers of the water column (Angelescu & Prenske, 1987) and its
101 behaviour and distribution seems to be strongly linked with the spatial structure of the
102 pelagic system (Wang *et al.* 2007; Ocampo Reinaldo *et al.* 2011).

103 In this context, the seasonality of the catch-per-unit-effort (CPUE) of hake
104 (Williams *et al.* 2010), together with the habits of the species and the strong
105 oceanographic processes in SMG (Gagliardini & Rivas, 2004), suggest there might be a
106 close relationship between the distribution of this species and the environmental cycles.

107 The aim of this study was to determine the relationship of the spatial-temporal
108 distribution of *Merluccius hubbsi* with the oceanographic processes in SMG. Also, the
109 seasonal effect of fishing on the hake population structure in relation to the formation of
110 the frontal system was analysed. The results are discussed in relation to the spatial
111 patterns and life cycle of the Argentine hake in SMG and the potential use of this
112 information for the design of management measures for the fishery.

113

114 Methods

115 *Study system: the environment and the fishery of Merluccius hubbsi.*

116 San Matías Gulf (40°50′-42°15′S and 63°05′-65°10′W, Figure 1) is the second largest
117 gulf in Argentina (about 20,000 km²) and is a semi-enclosed basin with a maximum
118 depth of 180 m in the central area (up to 55% of its total area is deeper than 100 m) and
119 the mouth, at the eastern side, with a depth of 50-70 m (Chart H214 Argentine Service
120 of Naval Hydrography; Williams *et al.* 2010). The northwest and southeast areas have
121 different characteristics, separated by a seasonal tidal front (October to April;

122 Gagliardini and Rivas 2004). The northern area of the gulf shows higher temperature
123 and salinity, with a strong thermocline, limited nitrate concentrations and a low turnover
124 rate of its waters. The southern area shows lower temperature and salinity, a lack of
125 stratification and a comparatively higher nitrate concentration (Rivas and Beier 1990).
126 The observed SST of the northern and southern areas, when the tidal front is present,
127 differs on average between 1 °C and 3 °C. During winter (May to September) the front
128 vanishes and the differences are less than 1 °C (Piola and Scasso 1988; Gagliardini &
129 Rivas 2004). The general circulation pattern in spring-summer is dominated by a
130 cyclonic gyre, located at the northern half of the basin (70 km diameter approximately,
131 Piola & Scasso 1998), which in combination with the frontal system determines the
132 relative isolation of the northern water masses (Rivas & Beier 1990, Tonini 2010).
133 The Argentine hake is very common throughout the ACS at depths ranging from 50 to
134 500 m (Cousseau & Perrotta 2004) and the stock located at the SMG constitutes a
135 unique independent demographic unit (Di Gi acomo *et al.* 1993; Sardella & Timi 2004;
136 Gonz alez *et al.* 2007; Machado Schiaffino *et al.* 2011). The population structure of this
137 stock seems to have been well preserved since the beginning of the fishery in 1971
138 (Romero *et al.* 2010; Ocampo Reinaldo 2010) compared with the ACS main stocks,
139 which are considered overexploited (Figure 1, Aubone *et al.* 2004; Vaz-dos-Santos *et*
140 *al.* 2010). In SMG, the Argentine hake spawns between August and March, with its
141 maximum activity during October and November, indicating the most important
142 reproductive schools are in the northern half of the basin (Di Gi acomo *et al.* 1993;
143 Ocampo Reinaldo 2010). This reproductive pattern led in 1998 to imposing a fishing
144 ban on the industrial fleet in October and November (Figure 1, Ministerial decision
145 555/2003, Ministry of Economy of R o Negro Province, Argentina).

146

147 *Environmental data*

148 Environmental data from remote sensing were obtained and validated following the
149 methods of Williams *et al.* (2010). Data from the Daily Level 1B local area coverage
150 (LAC) of the Advanced Very High Resolution Radiometer (AVHRR) on-board the
151 NOAA-N polar orbiting satellites and Sea-Viewing Wide Field of view Sensor
152 (SeaWiFS) were acquired through the Argentine National Commission of Space
153 Activities (CONAE). AVHRR data were obtained for the periods 2004–2007 and
154 SeaWiFS data for the period 2004-2006 (SeaWiFS images were available only up to 22
155 December 2006).

156 Relatively cloud-free AVHRR and SeaWiFS scenes were processed applying the
157 Multichannel Sea Surface Temperature (MCSST) (McClain *et al.* 1985) and OC4v4
158 algorithms (O'Reilly *et al.* 1998), respectively. AVHRR data were processed using
159 Erdas Imagine and SeaWiFS data using SeaWiFS Data Analysis System (SeaDAS)
160 version 5.2 (update#4) software (Baith *et al.* 2001). SST and Chl *a* were mapped to a
161 WGS 84 reference system (datum WGS84, ellipsoid WGS84), on the cartographic
162 Transverse Mercator projection (zone 4) at 1100 m of spatial resolution at nadir and co-
163 registered with respect to a reference landmask. Land and cloudy pixels were flagged to
164 zero and were not considered for the computations.

165 Monthly composites were created from the daily images, grouping all years and
166 resulting in 12 scenes. The number of cloud-free pixels contributing to each monthly
167 composite was spatially and temporally variable. The total numbers of cloud-free
168 images used to create the scenes are shown in Table 1.

169 SST gradients ($^{\circ}\text{C km}^{-1}$) were calculated from each monthly SST image by
170 applying a Sobel operator in a 5x5 window size (Simpson 1990). The Sobel operator
171 consist in two 5x5 convolution masks, which are used to calculate two images

172 containing approximations for derivatives (in west-east and north-south directions) and
173 assuming that there is an underlying continuous intensity function. At each pixel of the
174 image, gradient magnitudes are computed and the results show how "abruptly" or
175 "smoothly" the image changes at that pixel.

176 In order to evaluate the depths where the fleet operates, a topographic map of
177 SMG was obtained by natural neighbour interpolation (250 m resolution, resampled to
178 1100 m) (Schneider 2009) based on the nautical chart H214 of the Argentine Service of
179 Naval Hydrography.

180

181 *Fishing activity data*

182 The industrial bottom trawl fleet of SMG, which mainly target the Argentine hake, is
183 characterized by relatively small vessels (20 to 36 m length and 400 to 800 HP),
184 between 15 and 30 years old (Romero *et al.* 2007) that are fully capable of operating
185 along the entire SMG for up to 8-10 days without returning to port. Most fishing
186 captains are highly experienced local veterans. However, most of the catches are
187 obtained following a process of "trial and error" and the success of a fishing haul
188 generates repetitions within the same area. Conversely, a failed haul (i.e. a haul with a
189 small catch) motivates the search of a different area. This leads us to assume that the
190 fleet behaves as a relatively efficient predator and its persistence in an area is indicative
191 of the location of the largest concentrations of resources (at least those commercially
192 profitable). This approach allows us to infer the seasonal abundance of Argentine hake
193 in different areas of SMG.

194 Data of the bottom trawl fleet activity for the 2004–2007 period were obtained
195 from two different sources: 1) locations of hauls gathered by a Vessel Monitoring
196 System (VMS, named SiMPO (González *et al.* 2004)) and, 2) monthly landings and

197 fishing effort (to calculate the CPUE, in $\text{kg}\cdot\text{h}^{-1}$) obtained from official logbook records
198 of the Fishery Directorate of Río Negro province, Argentina (Millán 2007).

199 The SiMPO provided real-time data of vessel position, bearing and speed (every
200 96 minutes approximately) by on board Inmarsat D+ satellite transceivers. Criteria of
201 speed were used to discriminate the SiMPO records that corresponded to fishing
202 activities: records lower than 2.5 knots and higher than 4.0 knots were excluded, as they
203 were not associated with fishing activity. All data were inspected to remove additional
204 invalid records (e.g. speed at this range due to adverse weather conditions or port
205 arrivals). The validity of the filtering criteria was evaluated by comparing on board
206 observations of the duration of the hauls (Fisheries Observers Program of Río Negro
207 Province -FOP-) with records transmitted over the same hauls by the SiMPO.

208 Fishing activity data were plotted as topographic representations using the same
209 reference system of the environmental data. Data (counts of records per unit area) were
210 grouped monthly and a spatial smoothing was performed to represent the areas with the
211 highest fishing intensity. The smoothing was performed using a *Kernel density*
212 *interpolation* (ESRI ArcGIS Desktop version 9.3), which involves placing a
213 symmetrical surface over each point (records of fishing), evaluating the distance from
214 the point to a reference location (one pixel on the SST image) based on a mathematical
215 function, and summing the value of all the surfaces for the reference location. This
216 procedure was repeated for every reference locations.

217 The mathematical function of surface density used was the normal distribution,
218 according to:

219

220
$$CPUE_{sm} = g(x_j) = \sum \left\{ I_i * \frac{1}{1/(h^2 * 2\pi)} * e^{-\left(\frac{d_{ij}^2}{2 * h^2}\right)} \right\} \quad (1)$$

221

222 where $CPUE_{sm}$: smoothed $CPUE_{rec}$ that correspond to a particular pixel; d_{ij} : distance
223 between the reference location and any point within the search radius considered; h :
224 standard deviation of normal distribution (in this case the bandwidth or search radius);
225 I_i : intensity of each point. In this case, a scale value of $I_i = CPUE_{rec}$ was used, being

226

$$227 \quad I_i = CPUE_{rec} = (L_i/R_i) \quad (2)$$

228

229 where $CPUE_{rec}$ is a new variable defined by landings (kg) per record of fishing; L_i :
230 pooled total landings for each month for the entire 2004 – 2007 period; R_i : number of
231 fishing records grouped for each month for the years 2004 to 2007. The bandwidth was
232 2500 m, and densities were calculated in a regular grid of 1100 m on the side of the
233 square cell, consistent with the resolution of the satellite images used. Each monthly
234 fishing activity map obtained was compared with the corresponding SST and Chl a
235 monthly maps.

236

237 Also, topographic information obtained from the topographic map assign the
238 bottom depth to each fishing position. The resulting depth distributions were compared
239 using the Kolmogorov-Smirnov test for two independent samples, taking pairs of
240 consecutive months ($\alpha = 0.05$).

240

241 *Statistical analyses*

242 The data used for the statistical analyses were obtained over a polygonal area from the
243 mouth of the SMG to near its coastal line (9172 square pixels, 1100 m of spatial
244 resolution, Fig. 1). The pixels with Chl a , SST, $CPUE_{sm}$ and SST gradients data were
245 filtered and only pixels with data of all variables were used. The resulting pixels were

246 split into two datasets: Autumn-Winter (May to October, absence of the thermal front)
247 and spring-summer (November to April, with presence of the thermal front) (Williams
248 *et al.* 2010). The variable Chl *a* had fewer pixels with data (due to a higher number of
249 cloudy pixels), conditioning the selection up to 5167 pixels (56%) of total pixels
250 available. Multivariate Partial Mantel tests were performed for each dataset in order to
251 evaluate the general association between pairs of variables (Euclidean distance, 999
252 permutations, Bonferroni's corrected $\alpha=0.0084$). Also, the CPUE_{sm} and SST gradients
253 for the original 9172 pixels were categorized as "High", "Medium" and "Low" (Table
254 2), and a Pearson χ^2 test was performed for each month. The hypotheses of
255 independency were tested applying the Bonferroni's correction ($\alpha=0.042$).

256

257 *Additional biological and fishery information*

258 Data from quasi-monthly samples were obtained on board by the FOP, from commercial
259 catches (2004 to 2007). The monthly average sex ratio of *Merluccius hubbsi* catches
260 was calculated on the basis of the data obtained from each haul. In order to evaluate the
261 biological condition of the reproductive population of hake, gonadal stage and liver
262 weight were recorded in mature females (larger than 27 cm, Ocampo Reinaldo, 2010).
263 The hepatosomatic index (*HSI*) was calculated, as:

264

$$265 \quad HSI = 100 * (W_L / TW) \quad (3)$$

266

267 where W_L is the weight of the liver and TW is the total weight of the fish. Individual
268 results were averaged to obtain an overall value of *HSI* for each month.
269 Finally, monthly CPUE ($\text{kg} \cdot \text{h}^{-1}$) of the *M. hubbsi*, *Serirolella porosa* and other species

270 were grouped together and were analysed in order to describe the seasonal dynamics of
271 the fishery.

272

273 Results

274 Considering the high temporal resolution (12 h) and availability of images from
275 AVHRR sensors aboard NOAA satellites, 338 clouded-free images were obtained from
276 January 2004 to December 2007. On the other hand, 130 SeaWiFS clear daily images
277 were obtained from January 2004 to December 2006, because this sensor depends on
278 the daylight and is aboard the OrbView-2 satellite, which has a temporal resolution of
279 24 h (Table 1). Monthly climatological SST and SST gradients maps confirm the
280 presence of the frontal system during summer months (December to February) and its
281 absence during winter (May to August). During September and October, the front
282 begins to appear (increasing SST gradients), while in March and April it begins to
283 disappear (Figs 2a, b). SeaWiFS images indicates that the Chl *a* distribution from
284 December to February corresponds to the thermal front (Figure 2c): The warm waters of
285 the north matched with minimal Chl *a* concentrations, while the cold waters of the south
286 corresponded to higher Chl *a* concentrations.

287 The number of fishing records was in relation to the duration of the hauls and
288 false negative records were seldom detected (Figure 3), whereas scarce false-positive
289 records were totally discarded during *a priori* auditing.

290 The depth ranges of trawling remained largely between 80 and 160 m (Figure 4).
291 With the exception of February-March and May-June, the distribution of the hauls in
292 relation to the topography showed significant differences between consecutive months
293 (Kolmogorov-Smirnov, $\alpha=0.05$, Figure 4). During summer (December to March), the
294 highest activity of the fleet was concentrated in the southeast and southern areas of the

295 gulf, over (or near) the area of the thermal front (Figure 2d). The highest *Merluccius*
296 *hubbsi* yields (700-900 kg.h⁻¹) were obtained during this season (Figure 5) and females
297 outnumbered males in the catches (Figure 6).

298 During autumn-winter (April to September), yields of hake were lower (200-
299 400 kg.h⁻¹) and males were dominant in the catches. The female hake captured by the
300 fleet through the entire year showed rising gonadal maturation from January to
301 September. In October and November, spawning occurred (Figure 7) as well as in
302 December when an increase in post-spawning and gonadal recovery stages was
303 observed. In agreement with the gonadal cycle, an increase in *HSI* was detected towards
304 September, while from October it decreased to its lowest value in April (Figure 8).

305 Interestingly, from August to September, the fleet concentrated in the northern
306 part of the Gulf (with no frontal areas, Figure 2d) and catches of the silver warehou
307 *Seriolella porosa* rapidly increased, from almost null to a peak of 1000 kg.h⁻¹
308 approximately. Catches of silver warehou rapidly decreased in September (Figure
309 5). During spring (October and November) the fleet moved southwards due to the
310 implementation of the seasonal closure for the Argentine hake.

311 The remaining grouped species consisted mainly (up to 75-90%, in order of
312 importance) of plownose chimaera *Callorhynchus callorhynchus* (Linnaeus, 1758), mixed
313 species, the flounders *Xystreurys rasile* (Jordan, 1891) and *Paralichthys spp*, the
314 Patagonian hoki *Macruronus magellanicus* and the Parona leatherjacket *Parona signata*
315 (Jenyns, 1841). The yields of this group did not show significant variations throughout
316 the year, although in autumn-winter values were slightly higher.

317 The results of the Partial Mantel test showed that the variables Chl *a* and SST
318 are associated throughout the year, as well as SST and SST gradients (Table 3). On the
319 other hand, SST gradients were associated with Chl *a* in Spring-Summer and were not

320 associated in Autumn-Winter. The CPUE_{sm} was associated with SST and SST gradients
321 only in spring-summer (Table 3).

322 The categorized SST gradients and CPUE_{sm} were independent in May, June and
323 July (Pearson χ^2 test, $\alpha=0.0042$, Table 4), but the variables were dependent for the
324 remaining months.

325

326 Discussion

327 This study contributes to the understanding of the spatial patterns of *Merluccius*
328 *hubbsi* and its relations with the main oceanographic features of a semi-enclosed
329 Patagonian ecosystem. A strong seasonal oceanographic pattern was confirmed, in
330 accordance with the description by Gagliardini & Rivas (2004). According to Williams
331 *et al.* (2010, 2012), SST data in this study area showed a good correlation between
332 satellite-derived and *in situ* data . On the contrary, a poor correlation between *in situ*
333 and remotely sensed Chl *a* concentrations has been found. Although in these results, the
334 authors highlighted that the qualitative analysis revealed that AVHRR and SeaWiFS
335 images reproduced temporal and spatial variability of SST and Chl *a* data measured *in*
336 *situ* (Williams *et al.* 2010). Based on this information and the results of the SST and Chl
337 *a* climatological maps, two areas with different environmental characteristics were
338 confirmed in spring-summer: a warmer one in the northern area and a cooler one in the
339 southern area. The spatial distribution of SST and Chl *a* was related to the position
340 of this front in summer and the absence of the front in autumn-winter. These results are
341 consistent with previous studies (Piola & Scasso 1988; Gagliardini & Rivas 2004;
342 Williams *et al.* 2010), which reported two areas separated by a frontal system for most
343 of the year. Satellite chlorophyll data jointly with SST, have been used in several studies
344 to identify ecological regions in the ocean (e.g. Herut *et al.* 2000; Polovina *et al.* 2001;

345 More & Abbott 2002; Zainuddin *et al.* 2006). Generally, these ecological regions are
346 not fixed in time or space and vary seasonally (Stuart *et al.* 2011). The results of this
347 study showed a strong spatial association between SST and Chl *a* throughout the year
348 suggesting that the satellite-derived SST data (abundant, easy to obtain and more
349 reliable) might be used as a rough proxy to infer the spatial (superficial) structure of
350 different waters masses in SMG (particularly in winter when the satellite-derived Chl *a*
351 data is fragmentary). In general, the seasonal variability of the monthly values of
352 satellite-derived Chl *a* for the whole area of GSM show average concentrations during
353 autumn-winter, a peak in early spring (September) and the lowest Chl *a* values during
354 summer (Williams *et al.* 2012). This seasonal cycle of the SMG is characteristic of
355 subtropical waters (Mann and Lazier 1996, Williams *et al.* 2012).

356 Comparisons between SST gradient maps and the fishing activity maps showed
357 that the fishing fleet was concentrated over and near the area of the frontal system
358 during summer (December to March), obtaining the highest CPUE of the Argentine
359 hake in relatively deep waters. Since the Argentine hake is the most important resource
360 for the local industry, the dispersion of the fleet in autumn could be due to a reduction in
361 CPUE, which would encourage captains to seek better catches in other (shallower)
362 areas. The dispersion of the fleet coincides with the dissipation of the front, suggesting
363 that the distribution and shoaling of the Argentine hake is associated with the presence
364 of this tidal front. The explanation could be that the fronts increase the vertical
365 mixing of water (Mann & Lazier 1996), resulting in increased primary productivity and,
366 in some cases, in the activity of higher trophic levels (Olson & Backus 1985; Acha *et al.*
367 2004). Moreover, considering that adult hake feed actively after spawning (Hart 1946
368 *sensu* Podestá 1989), the formation of the front probably allows dense shoals to feed

369 after the spawning season, recovering energy and the lipids reserves used during the
370 reproductive season (Angelescu & Prenski 1987).

371 As mentioned before, the fleet remained dispersed in relatively shallow areas in
372 autumn-winter, until the abrupt increase in catches of silver warehou *Serirolella porosa*
373 in deep waters in the north of the gulf. The silver warehou is a typically pelagic and
374 coastal species that is rarely found below 100 meters depth (Cousseau & Perrota 2004).
375 This species has become the second important species in landings since 1998, due to a
376 combination of seasonal appearance of dense shoals and commercial opportunities
377 (Romero 2011). In this study, an increase in the number of hauls was observed between
378 August and September, because fishermen performed night hauls to take advantage of
379 the abundance of the silver warehou (Ocampo Reinaldo, 2010). Unfortunately, there is a
380 lack of information about the biology and ecology of this species. The causes of the
381 seasonal occurrence of the silver warehou within the gulf, as well as its apparent
382 disappearance in late September remains unknown. The massive shoaling of the silver
383 warehou seems to be related to a reproductive response (Ocampo Reinaldo, 2010) and
384 not to the environmental features analysed in this study. Related to this, the statistical
385 dependence between $CPUE_{sm}$ (constituted mainly by silver warehou) and SST gradients
386 during August and September, could be explained by a large number of pixels with a
387 combination of “Low gradients” and “High $CPUE_{sm}$ ” (Figure 9).

388 The “other species” group did not show significant variations throughout the
389 year and the slight increase in winter yields may be due to: 1) a greater diversity of fish
390 species in winter fishing areas (shallow waters), or 2) fishermen found a better
391 commercial use of the bycatch, because of a lack of target species.

392 The oceanographic processes observed in this study allow us to infer some
393 aspects of the spatial patterns of the Argentine hake. The winter decreases in CPUE may

394 be explained by the dispersion of individuals (searching for food) throughout the water
395 column in response to the absence of an environmental structure of the water.
396 Moreover, some pelagic species are important prey in the diet of the Argentine hake of
397 all sizes (e.g. Euphausiidae and anchovy *Engraulis anchoita* Hubbs & Marini, 1935;
398 Ocampo Reinaldo *et al.* 2011) and prey aggregations can be related
399 to surface environmental parameters (Alemany *et al.* 2009; Spinelli *et al.* 2012), thus the
400 distribution of hake may be coupled, in part, with the distribution of their prey.

401 It is widely known that fish larvae should hatch into a realm with appropriate
402 food and benign abiotic conditions (Hjort 1914; Cushing 1975, Lasker 1975; Bakun
403 1996; Gotceitas *et al.* 1996; Bakun & Csirke 1998). Moreover, the timing of spawning
404 is decisive, particularly in areas with large seasonal changes in temperature and daylight
405 hours (Wootton 1998). The spawning of the Argentine hake coincides with the seasonal
406 structure of the water masses (warmer and stratified waters) in the northern area of
407 SMG, which creates positive conditions to concentrate food, serving as favourable first-
408 feeding sites for fish larvae (Bakun 1996). Therefore, the thermocline and
409 environmental conditions should contribute to the timing of spawning of Argentine hake
410 (González *et al.* 2010), and these areas could act as holding areas for eggs and larvae
411 enhancing the reproductive success (Iles and Sinclair 1982; Macchi *et al.* 2004).
412 Accordingly, the formation of the thermal front and the environmental patterns observed
413 in this study may lead and modulate the reproductive strategy of the Argentine hake in
414 SMG and the successful retention of hake recruits. In addition, the general circulation
415 pattern of SMG in spring-summer is dominated by a cyclonic gyre, located at the
416 northern half of the basin (Piola & Scasso 1998), which, in combination with the frontal
417 system, determines the relative isolation of the northern water masses. The relative
418 isolation of the northern waters contributes to the retention up to 40% of pelagic

419 particles in the pelagic dominion over 250 days (Tonini 2010). This phenomenon may
420 promote the retention of eggs and larvae of hake, as well as other planktonic organisms
421 on the basis of the trophic chains (i.e. Euphausiidae), which are the main source of food
422 for fish at larval and post-larval stages (Spinelli *et al.* 2012). Overall, the oceanographic
423 characteristics of SMG seem to explain the summer distribution pattern of the Argentine
424 hake, which may adapt its reproductive strategy and foraging behaviour to the cyclic
425 environmental processes observed in the gulf. In contrast, on the ACS (outside the
426 SMG), the “northern stock” spawns over the entire year, with peaks of activity from
427 May to July (Rodrigues & Macchi 2010), whereas the “Patagonian stock” spawns from
428 November to March, with peaks in January (Macchi *et al.* 2004). In upwelling zones,
429 the Chilean hake *Merluccius gayi*, for example, spawns in association with frontal
430 structures to enhance offspring survival (Vargas & Castro 2001), whereas the drift
431 patterns of early larvae of the European hake *Merluccius merluccius* are a consequence
432 of the local hydrographical processes (Alvarez *et al.* 2001; Olivar *et al.* 2003). In this
433 respect, the duration of the pelagic larval phase of the Argentine hake is around 65 days
434 (Buratti & Santos 2010). Therefore, the timing of spawning, the oceanographic
435 phenomena and the topography observed in SMG seem to explain the isolation of this
436 stock, supporting various new hypotheses about the importance of the Patagonian gulfs
437 in the conservation of the aquatic resources (Machado Schiaffino *et al.* 2011).

438 Tidal fronts are relatively short temporal scale systems, which have been shown
439 to have a stronger influence on fish diversity, biomass and assemblage structure than
440 permanent frontal areas (Alemany *et al.* 2009). Accordingly, our results showed that the
441 absence of a water mass structure in cold months does not promote the shoaling of hake,
442 which is reflected in the dispersal of the fishing fleet and low landings. Considering that
443 there is a seasonal ban that protects the reproductive process of hake, it is interesting to

444 point out that the fleet captured a higher proportion of females in gonadal recovery stage
445 in the warm months (after the seasonal ban, outside the closure area), obtaining the
446 highest CPUE of the year. Although the winter catches showed mainly males and a low
447 CPUE, the intense summer fishing may result in a high impact on the female
448 population. This information is relevant to the design of new management tools (e.g.
449 closures over the frontal zone or effort restrictions in summer) intended to provide
450 biological sustainability to the Argentine hake fishery. It has been proposed that the
451 ability of a population to rebuild itself in a closed area may depend on the fishing effort
452 in that area before the closure (Babcock *et al.* 2005). However, it is also important to
453 consider the effect of the displaced effort and, particularly in SMG, the seasonal
454 concentration of fishing effort in the front area over segregated shoals of female hake.

455 Remote sensors are excellent tools to complement biological information with
456 large-scale environmental information (Platt *et al.* 2007; Stuart *et al.* 2011). Vessel
457 Monitoring System data are appropriate for mapping the large-scale distribution of
458 fishing effort and the area impacted (Gerritsen & Lordan 2011; Skaar *et al.* 2011; Saitoh
459 *et al.* 2011). In this study, a generalized approach (VMS and landing records) was used
460 to identify the areas of SMG where trawlers seasonally operate and to analyse the
461 potential relationships between abundance of the species captured and oceanographic
462 processes.

463 Future research should focus in obtaining more *in situ* data about the seasonal
464 distribution and abundance of species of intermediate trophic levels, as well as data of
465 primary production, consumption and trophic relationships in the area of the frontal
466 system. This information will contribute to a better understanding of the ecological
467 processes that underlie the observed relationships between the physical ecosystem and
468 fishery resources. Finally, the spatial management could be an interesting

469 complementary tool and may enhance the expected effects of non-spatial strategies,
470 helping to prevent biases in trends caused by spatial heterogeneity of populations and
471 communities (Babcock *et al.* 2005), and supporting the gradual development of
472 ecosystem-based fishery management.

473

474 Acknowledgements

475 The authors thank M. Sapoznik and N. Pérez de la Torre for their assistance in the
476 processing of satellite images; P. Osovnikar and M. Maggioni for logistics of sampling;
477 Cesar García and Ingrid Teich for their assistance in the spatial analyses and anonymous
478 referees for their critical reviews and suggested changes to the manuscript. M.O.R.,
479 G.W, L.S and M.A.R. were supported by fellowships of CONICET (Argentina) and the
480 work was partially supported by the projects PID 2003 371 and PICT 2006 1575
481 (ANPCyT, Argentina).

482

483 References

484 Acha, E.M., Mianzan, H.W., Guerrero, R.A., Favero, M., Bava, J. 2004. Marine fronts
485 at the continental shelves of austral South America, physical and ecological processes.
486 *Journal of Marine Systems* 44: 83–105.

487 Alemany, D., Acha, E.M., Iribarne, O. 2009. The relationship between marine fronts
488 and fish biodiversity in the Patagonian Shelf Large Marine Ecosystem. *Journal of*
489 *Biogeography* 36: 2111–2124.

490 Alvarez, P., Motos, L., Uriarte, A., Egaña, J. 2001. Spatial and temporal distribution of
491 European hake, *Merluccius merluccius* (L.), eggs and larvae in relation to
492 hydrographical conditions in the Bay of Biscay. *Fisheries Research* 50: 111-128.

493 Aminot, A., Guillaud, J., Kkrouel, R. 1998. Apports de nutriments et développement
494 phytoplanctonique en baie de Seine. *Oceanologica Acta* 21: 923-935

495 Angelescu, V., Prenski, L.B. 1987. Ecología trófica de la merluza común del Mar
496 Argentino (Merlucciidae, *Merluccius hubbsi*). Parte 2. Dinámica de la alimentación
497 analizada sobre la base de las condiciones ambientales, la estructura y las evaluaciones
498 de los efectivos en su área de distribución. Contribución INIDEP 561. 205 pp.

499 Aubone, A., Bezzi, S. I., Cañete, G., Castrucci, R., Dato, C., Irusta, G., Madirolas, A.,
500 Perez, M., Renzi, M., Santos, B., Simonazzi, M., Villarino, M. F. 2004. Evaluación y
501 sugerencias de manejo del recurso merluza (*Merluccius hubbsi*). La situación hasta
502 1999. In Sánchez R. P., Bezzi S.I., editors. *El Mar Argentino y sus recursos pesqueros*,
503 Tomo 4. Mar del Plata: INIDEP, pp. 207–235.

504 Babcock, E. A., Pikitch, E. K., McAllister, M. K., Apostolaki, P., Santora, C. 2005. A
505 perspective on the use of spatialized indicators for ecosystem-based fishery
506 management through spatial zoning. *ICES Journal of Marine Science* 62: 469-476.

507 Baith K., Lindsay, R., Fu, G., McClain, C.R. (2000) SeaDAS: data analysis system for
508 ocean color satellite sensors. *Eos Transactions American Geophysical Union* 82: 202.

509 Bakun, A. 1996. *Patterns in the ocean: Ocean processes and marine population*
510 *dynamics*. California: California Sea Grant College System, NOAA, 341 pp.

511 Bakun, A., Csirke, J. 1998. Environmental processes and recruitment variability. In
512 Rodhouse P. G., Dawe E. G., O'Dor R. K., editors. Squid recruitment dynamics. Roma:
513 FAO, pp 105-124.

514 Ballance, L., Pitman, M., Reilly, S.B. 1997. Seabird community structure along a
515 productivity gradient: Importance of competition and energetic constraint. *Ecology* 78:
516 1502-1518.

517 Buratti, C.C., Santos, B.A. 2010. Otolith microstructure and pelagic larval duration in
518 two stocks of the Argentine hake, *Merluccius hubbsi*. *Fisheries Research* 106: 2–7

519 Cousseau, M.B., Perrotta, R.G. 2004. Peces Marinos de Argentina. Biología,
520 distribución, pesca. Publicaciones Especiales Mar del Plata: INIDEP. 167 pp.

521 Cushing, D.H. 1975. Marine ecology and fisheries. London: Cambridge University
522 Press. 292 pp.

523 Di Giacomo, E.; Calvo, J.; Perier, M. R., Morriconi, E.R. 1993. Spawning aggregations
524 of *Merluccius hubbsi*, in patagonian waters: evidence for a single stock? *Fisheries*
525 *Research* 16: 9-16.

526 Druon, J., Fromentin, J., Aulanier, F., Heikkonen, J. 2011. Potential feeding and
527 spawning habitats of Atlantic bluefin tuna in the Mediterranean Sea. *Marine Ecology*
528 *Progress Series* 439: 223-240.

529 Friedland, K.D., Ahrenholz, D.W, Guthrie, J.F. 1996. Formation and seasonal evolution
530 of Atlantic Menhaden Juvenile Nurseries in Coastal Estuaries. *Estuaries* 19: 105-114.

531 Gagliardini, D. A., Rivas, A. L. 2004. Environmental characteristics of San Matías gulf
532 obtained from Landsat-TM and ETM+ data. *Gayana* 68: 186–193.

533 Gerritsen, H., Lordan, C. 2011. Integrating vessel monitoring systems (VMS) data with
534 daily catch data from logbooks to explore the spatial distribution of catch and effort at
535 high resolution. *ICES Journal of Marine Science* 68: 245-252.

536 González, R., Gaspar, C., Curtolo, L., Sangiuliano, I., Osovnikar P., Borsetta, N. 2004.
537 Fishery and Oceanographic Monitoring System (FOMS): a new technological tool
538 based on remote sensing, with application in ecosystem management of coastal fisheries
539 in Patagonia. *Gayana* 68: 234-238.

540 González, R., Narvarte, M., Caille, G.M. 2007. An assessment of the sustainability of
541 the hake *Merluccius hubbsi* artisanal fishery in San Matías Gulf, Patagonia, Argentina.
542 *Fisheries Research* 87: 58-67.

543 González, R., Ocampo Reinaldo, M., Schneider, C., Romero, M.A., Maggioni, M.,
544 Williams, G., Cabrera, G., Narvarte, M., Gagliardini, A. 2010. Correlating SST Satellite
545 Data to the Spatial Distribution of Spawning Aggregations of Argentine Hake
546 (*Merluccius hubbsi*) in San Matías Gulf, Patagonia, Argentina. In Barale V., Gower J.,
547 Alberotanza L., editors. *Proceedings of Oceans from Space Symposium 2010*. Joint
548 Research Centre, European Commission: JRC Scientific and Technical Reports
549 N°57986: 103-104.

550 Gotceitas, V., Puvanendran, V., Leader, L.L., Brown, J.A. 1996. An experimental
551 investigation of the 'match/mismatch' hypothesis using larval Atlantic cod. *Marine*
552 *Ecology Progress Series* 130: 29-37.

553 Hart, T.J. 1946. Report on trawling surveys on the Patagonian continental shelf.
554 Discovery Reports 23: 227-408.

555 Herut, B., Almogi-Labin, A., Jannink, N., Gertman, I. 2000. The seasonal dynamics of
556 nutrient and chlorophyll-*a* concentrations on the SE Mediterranean shelf slope.
557 Oceanologica Acta 23: 771-782.

558 Hjort, J. 1914. Fluctuations in the great fisheries of northern Europe. Procès-Verbaux
559 des Réunions du Conseil International pour l'Exploration de la Mer 20: 1-228.

560 Houde E. D. 2009. Recruitment variability. In Jakobsen T., Fogarty M. F., Megrey B.
561 A., Moksness E., editors. Fish reproductive biology: Implications for assessment and
562 management. London: Wiley-Blackwell, 91-171 pp.

563 Huot, Y., Babin M., Bruyant, F., Grob, C., Twardowski, M.S., Claustre, H. 2007.
564 Relationship between photosynthetic parameters and different proxies of phytoplankton
565 biomass in the subtropical ocean. Biogeosciences 4: 853-868.

566 Iles, T. D., Sinclair, M. 1982. Atlantic herring: Stock discreteness and abundances.
567 Science 215: 627-633.

568 Jaquet N., Whitehead, H., Lewis, M. 1996. Coherence between 19th century sperm
569 whale distributions and satellite-derived pigments in the tropical Pacific. Marine
570 Ecology Progress Series 145:1-10.

571 Lasker, R. 1975. Field criteria for survival of anchovy larvae: the relation between
572 inshore chlorophyll maximum layers and successful first feeding. Fishery Bulletin 73:
573 453-462.

574 Laurs, R.M., Fiedler, P.C., Montgomery, D.R. 1984. Albacore tuna catch distributions
575 relative to environmental features observed from satellite. *Deep Sea Research* 31: 1085-
576 1099.

577 Macchi, C.J., Pájaro, M., Ehrlich, M. 2004. Seasonal egg production pattern of the
578 Patagonian stock of Argentine hake (*Merluccius hubbsi*). *Fisheries Research* 67: 25–38.

579 Machado Schiaffino, G., Juanes, F., Garcia-Vazquez, E. 2011. Identifying unique
580 populations in long-dispersal marine species: Gulfs as priority conservation areas.
581 *Biological Conservation* 144: 330-338

582 Mann K. H. 1992. Physical influences on biological processes: how important are they?
583 *South African Journal of Marine Science* 12: 107-121.

584 Mann, K.H., Lazier, J.R.N. 1996. Dynamics of Marine Ecosystems. Biological-
585 Physical Interactions in the Oceans. USA: Blackwell Publishing. 496 pp.

586 McClain, E. P., Pichel, W.G., Walton, C.C. 1985. Comparative performance of
587 AVHRR-based multichannel sea surface temperature. *Journal of Geophysical Research*
588 90: 11587-11601

589 Millán, D. 2007. Anuario de Estadísticas Pesqueras de la Provincia de Río Negro.
590 Departamento de Policía de Pesca, Dirección de Pesca. Argentina.

591 Moore, J. K., Abbott, M. R. 2002. Surface chlorophyll concentrations in relation to the
592 Antarctic Polar Front: seasonal and spatial patterns from satellite observations. *Journal*
593 *of Geophysical Research* 37, 69-86.

594 Morel, A., André, J.M. 1991. Pigment Distribution and Primary Production in the
595 Western Mediterranean as Derived and Modelled From Coastal Zone Color Scanner
596 Observations. *Journal of Geophysical Research* 96: 685–12.

597 Ocampo Reinaldo, M. 2010. Evaluación pesquera integral de la merluza común
598 (*Merluccius hubbsi* Marini, 1933) del Golfo San Matías y efectos de la explotación de
599 esta especie sobre otros componentes de la trama trófica. Doctoral Thesis, National
600 University of Córdoba. 164 pp.

601 Ocampo Reinaldo, M., González, R. A., Romero, M. A. 2011 Feeding strategy and
602 cannibalism of the Argentine hake. *Journal of Fish Biology* 79: 1795–1814.

603 Olivar, M.P., Quílez, G., Emelianov, M. 2003. Spatial and temporal distribution and
604 abundance of European hake, *Merluccius merluccius*, eggs and larvae in the Catalan
605 coast (NW Mediterranean). *Fisheries Research* 60: 321–331

606 Olson, D.B. & Backus. R.H. 1985. The concentrating of organisms at fronts: a cold-
607 water fish and a warm-core Gulf Stream ring. *Journal of Marine Research* 43: 113-137.

608 O'Reilly J.E., Maritorena, S., Siegel, D., O'Brien, M., Toole, D., Greg Mitchell, B.,
609 Kahru, M., Chavez, F., Strutton, P., Cota, G., Hooker, S., McClain, C., Carder, K.,
610 Muller-Karger, F., Harding, L., Magnuson, A., Phinney, D., Moore, G., Aiken, J.,
611 Arrigo, K., Letelier R., Culver, M. 2000. Ocean color chlorophyll-*a* algorithms for
612 SeaWiFS, OC2, and OC4: Version 4. In Hooker S. B., Firestone E. R., editors.
613 SeaWiFS Postlaunch Calibration and Validation Analyses, Part 3. NASA Tech. Memo.
614 2000-206892. Maryland: NASA Goddard Space Flight Center, 11: 9-23.

615 Perrota R. G., Viñas, M. D., Hernández, D. R., Tringali, L. 2001. Temperature
616 conditions in the Argentine chub mackerel (*Scomber japonicus*) fishing ground:
617 implications for fishery management. *Fisheries Oceanography* 10: 275-283.

618 Piola, A. R., Scasso, L. M. 1988. Circulación en el Golfo San Matías. *Geoacta* 15: 33–
619 51.

620 Platt, T., Sathyendranath, S., Fuentes-Yaco, C. 2007. Biological oceanography and
621 fisheries management: perspective after 10 years. *ICES Journal of Marine Science* 64:
622 863–869.

623 Podestá, G.P. 1989. Migratory pattern of Argentine hake *Merluccius hubbsi* and oceanic
624 processes in the southwestern Atlantic Ocean. *Fishery Bulletin* 88: 167–177.

625 Polovina, J. J., Howell, E., Kobayashi, D. R., Seki, M. P. 2001. The transition zone
626 chlorophyll front, a dynamic global feature defining migration and forage habitat for
627 marine resources. *Progress in Oceanography* 49: 469–483.

628 Reddy R., Lyne, V, Randall, G., Eston, A., Clarke, S. 1995. An application of satellite
629 derived sea surface temperatures to southern bluefin tuna and albacore off Tasmania,
630 Australia. *Scientia Marina* 59: 445-45.

631 Rivas, A.L., Beier, E.J. 1990. Temperature and salinity fields in the Northpatagonic
632 Gulfs. *Oceanologica Acta* 13: 15-20.

633 Rodrigues, K.A, Macchi, G.G. 2010. Spawning and reproductive potential of the
634 Northern stock of Argentine hake (*Merluccius hubbsi*). *Fisheries Research* 106, 560–
635 566

636 Romero, M. A., González, R., Ocampo Reinaldo, M. 2010. When conventional fisheries
637 management measures are not effective to reduce the catch and discard of juvenile fish:
638 a case study of Argentine hake trawl fishery in San Matías Gulf (Patagonia, Argentina).
639 *North American Journal of Fisheries Management* 30: 702–712.

640 Romero, M.A. 2011. Rol de los mamíferos marinos en el contexto de la trama trófica
641 del ecosistema del Golfo San Matías e interacciones con las pesquerías de especies
642 demersales. Doctoral Thesis. National University of Comahue. 256 pp.

643 Romero, M. A., González, R., Zaidman, P., Millán, D. 2007. Síntesis histórica.
644 Estadísticas de desembarcos pesqueros, artesanales e industriales del Golfo San Matías,
645 Río Negro. *IBMP Serie Publicaciones* 7: 23–38.

646 Sabatini M., Martos, P. 2002. Mesozooplankton features in a frontal area off northern
647 Patagonia (Argentina) during spring 1995 and 1998. *Scientia Marina* 66: 215-232.

648 Saitoh, S-I., Mugo, R., Radiarta, I N., Asaga, S., Takahashi, F., Hirawake, T., Ishikawa,
649 Y., Awaji, T., In, T. and Shima, S. 2011. Some operational uses of satellite remote
650 sensing and marine GIS for sustainable fisheries and aquaculture. *ICES Journal of*
651 *Marine Science* 68: 687–695.

652 Sardella, N., Timi, J. 2004. Parasites of Argentine hake in the Argentine Sea: population
653 and infracommunity structure as evidence for host stock discrimination. *Journal Fish*
654 *Biology* 65: 1472–1488.

655 Schneider, C. 2009. Sistema de Composición Cartográfica del Instituto de Biología
656 Marina y Pesquera Alte. Storni. San Antonio Oeste: IBMPAS. 79 pp.

657 Simpson, J.J. 1990. On the accurate detection and enhancement of oceanic features
658 observed in satellite data. *Remote Sensing of Environment* 33: 17-33.

659 Skaar, K. L., Jørgensen, T., Ulvestad, B. K. H., Engås, A. 2011. Accuracy of VMS data
660 from Norwegian demersal stern trawlers for estimating trawled areas in the Barents Sea.
661 *ICES Journal of Marine Science* 68: 1615-1620.

662 Spinelli M.L., Pájaro M., Martos P., Esnal G.B., Sabatini M., Capitanio F.L. 2011.
663 Potential zooplankton preys (Copepoda and Appendicularia) for *Engraulis anchoita* in
664 relation to early larval and spawning distributions in the Patagonian frontal system (SW
665 Atlantic Ocean). *Scientia Marina* 76: 39-47.

666 Stuart, V., Platt, T., Sathyendranath, S. 2011. The future of fisheries science in
667 management: a remote-sensing perspective. *ICES Journal of Marine Science* 68: 644–
668 650.

669 Tonini, M. H. 2010. Modelado Numérico del Ecosistema de los Gofos Norpatagónicos.
670 Doctoral thesis. National University of Bahía Blanca. 265 pp.

671 Vargas, C.A., Castro, L.R. 2001. Spawning of the chilean hake (*Merluccius gayi*) in the
672 upwelling system off Talcahuano in relation to oceanographic features. *Scientia Marina*
673 65: 101-110.

674 Vaz-dos-Santos, A. M., Rossi-Wongtschowski, C. L. D. B., de Figueiredo, J. L., Ávila-
675 da-Silva, A. O. (2010) Threatened fish of the world: *Merluccius hubbsi* Marini, 1933
676 (Merlucciidae). *Environmental Biology of Fishes* 87: 349–350.

677 Wang J., Pierce G.J., Sacau M., Portela J., Santos M.B., Cardoso X., Bellido J.M. 2007.
678 Remotely sensed local oceanic thermal features and their influence on the distribution of
679 hake (*Merluccius hubbsi*) at the Patagonian shelf edge in the SW Atlantic. Fisheries
680 Research 83: 133-144.

681 Wehrtmann, I.S. 1994. Larval production of the caridean shrimp, *Crangon*
682 *septemspinosa*, in waters adjacent to Chesapeake Bay in relation to oceanographic
683 conditions. Estuaries 17: 509-518.

684 Williams G. N., Sapoznik, M., Ocampo Reinaldo, M., Solís, M., Narvarte, M.,
685 González, R., Esteves, J.L., Gagliardini, D.A. 2010. Comparison of AVHRR and
686 SeaWiFS imagery with fishing activity and in-situ data in San Matias Gulf, Argentina.
687 International Journal of Remote Sensing 31: 17-18.

688 Williams, G. N., Dogliotti A. I., Zaidman,P.; Solis, M.; Narvarte, M.; González, R.;
689 Esteves, J.L.; Gagliardini, D.A. 2012. Assessment of remotely-sensed sea-surface
690 temperature and chlorophyll-*a* concentration in San Matías Gulf (Patagonia, Argentina).
691 Continental Shelf Research. <http://dx.doi.org/10.1016/j.csr.2012.08.014>.

692 Wootton, R. J. 1998. Ecology of Teleost Fishes. London: Chapman and Hall. 404 pp.

693 Zainuddin M., Kiyofuji H., Saitoh K., Saitoh S.-I. 2006. Using multi-sensor satellite
694 remote sensing and catch data to detect ocean hot spots for albacore (*Thunnus alalunga*)
695 in the northwestern North Pacific. Deep-Sea Research Part II: Topical Studies in
696 Oceanography 53, 419-431.

697

698 TABLES

699 Table 1: Images free of clouds per month obtained from AVHRR (from 2004 to 2007)
 700 and SeaWiFS (from 2004 to 2006).

| Month | May | Jun | Jul | Aug | Sep | Oct | Nov | Dec | Jan | Feb | Mar | Apr |
|----------------|-----|-----|-----|-----|-----|-----|-----|-----|-----|-----|-----|-----|
| AVHRR | 12 | 25 | 33 | 15 | 31 | 19 | 36 | 39 | 39 | 35 | 36 | 18 |
| <u>SeaWiFS</u> | 4 | 2 | 2 | 6 | 16 | 15 | 12 | 11 | 23 | 16 | 13 | 10 |

701

702 Table 2: Categorized variables used in the test of independency. The pixels with SST
 703 gradients >0.1 in the SMG have been described as “frontal pixels” (Williams et al.
 704 2010).

| Categories | SST gradients | CPUE _{sm} |
|---------------|---------------|--------------------|
| High | >0.1 | >1000 |
| Medium | 0.05-0.1 | 500-1000 |
| Low | <0.05 | <500 |

705

706 Table 3: Results of the Partial Mantel test (Euclidean distance, 999 permutations,
 707 Bonferroni’s corrected $\alpha=0.0084$). The variables used to calculate the first and second
 708 distance matrix are shown. The third distance matrix used in all analyses was based in
 709 the geographical position of each pixel. Significant tests are shown in bold and p values
 710 between parentheses.

| Autumn/Winter | SST | <u>Chl a</u> | <u>SST_{grad}</u> | CPUE _{sm} | Spring/Summer |
|---------------------------|-----------------------|-----------------------|---------------------------|------------------------|---------------------------|
| SST | | 0.7885 (0.001) | 0.1731 (0.001) | 0.01937 (0.005) | SST |
| <u>Chl a</u> | 0.1854 (0.001) | | 0.2118 (0.001) | 0.0084 (0.069) | <u>Chl a</u> |
| <u>SST_{grad}</u> | 0.2622 (0.001) | -0.0482 (1) | | 0.1102 (0.001) | <u>SST_{grad}</u> |
| CPUE _{sm} | -0.04173 (1) | 0.0011 (0.406) | -0.1019 (1) | | CPUE _{sm} |

711

712 Table 4: Results of the Pearson χ^2 test of independency between CPUEsm and SST
 713 gradients (3x3 table, Bonferroni's corrected $\alpha=0.0042$). Significant tests are shown in
 714 bold.

| Month | May | Jun | Jul | Aug | Sep | Oct | Nov | Dec | Jan | Feb | Mar | Apr |
|------------------|--------|--------|--------|--------------|--------------|--------------|---------------|--------------|--------------|---------------|---------------|--------------|
| χ^2 Pearson | 11,77 | 6,46 | 11,28 | 47,48 | 63,48 | 19,58 | 194,86 | 28,96 | 49.49 | 209,71 | 122,15 | 32,57 |
| <i>p</i> | 0,0191 | 0,1676 | 0,0236 | <0,0001 | <0,0001 | 0,0006 | <0,0001 | <0,0001 | <0,0001 | <0,0001 | <0,0001 | <0,0001 |

715

716 FIGURE CAPTIONS

717 Figure 1: Location of the three stocks of *Merluccius hubbsi* in Argentine waters. There
718 are 2 closure areas for trawlers in SMG (Río Negro Province): a seasonal one from
719 October to November at north of parallel $41^{\circ}30'S$, and a permanent one (small
720 polygon), which is an area reserved for artisanal longliners. The figure shows the
721 relative position of the tidal front and the general circulation in the basin during
722 summer. The big polygon (dotted line) shows the area sampled for the statistical
723 analyses. NS: Northern stock; PS: Patagonian stock.

724

725 Figure 2: Monthly climatological maps and fishing activity maps of the SMG. a) SST;
726 b) SST gradients, c) Chl a, d) fishing activity.

727

728 Figure 3: Frequency of fishing activity records from the SiMPO respect to the duration
729 of the hauls registered by the FOP. 0: False negative (The SiMPO failure to register the
730 fishing activity). 1, 2, 3: Indicate the number of SiMPO records per haul. The z-axis
731 labels were rearranged to facilitate interpretation.

732

733 Figure 4: Frequency distribution of the fishing depths of the SiMPO registers. The
734 letters (a, b) indicate months without statistical differences between them (Kolmogorov-
735 Smirnov, $\alpha=0.05$). ad: Average depth; se: standard error.

736

737 Figure 5: Monthly CPUE of *Merluccius hubbsi*, *Serirolella porosa* and other species,
738 grouped from 2004 to 2007. The largest effort (dotted line) was registered in August
739 and September, because the fleet added additional night hauls to catch more silver
740 warehou.

741

742 Figura 6: Average proportion of sexes in the catch of *Merluccius hubbsi* (number of
743 females/number of males) per month, grouped for the years 2004 to 2007. Months have
744 been distinguished with the presence of seasonal thermal front. The x-axis labels
745 indicate the month of capture, the total number of individuals sampled and the number
746 of hauls from which these individuals have been obtained.

747

748 Figure 7: Gonadal stages of mature females of *Merluccius hubbsi* (>27 cm of total
749 length) in monthly catches of the industrial fleet. The x-axis labels indicate the month of
750 capture, the total number of individuals sampled and the number of hauls from which
751 these individuals have been obtained. 1, 2, 3 and 4: Pre-spawning stages; 5: spawning, 6
752 and 7: post-spawning and gonadal recovery.

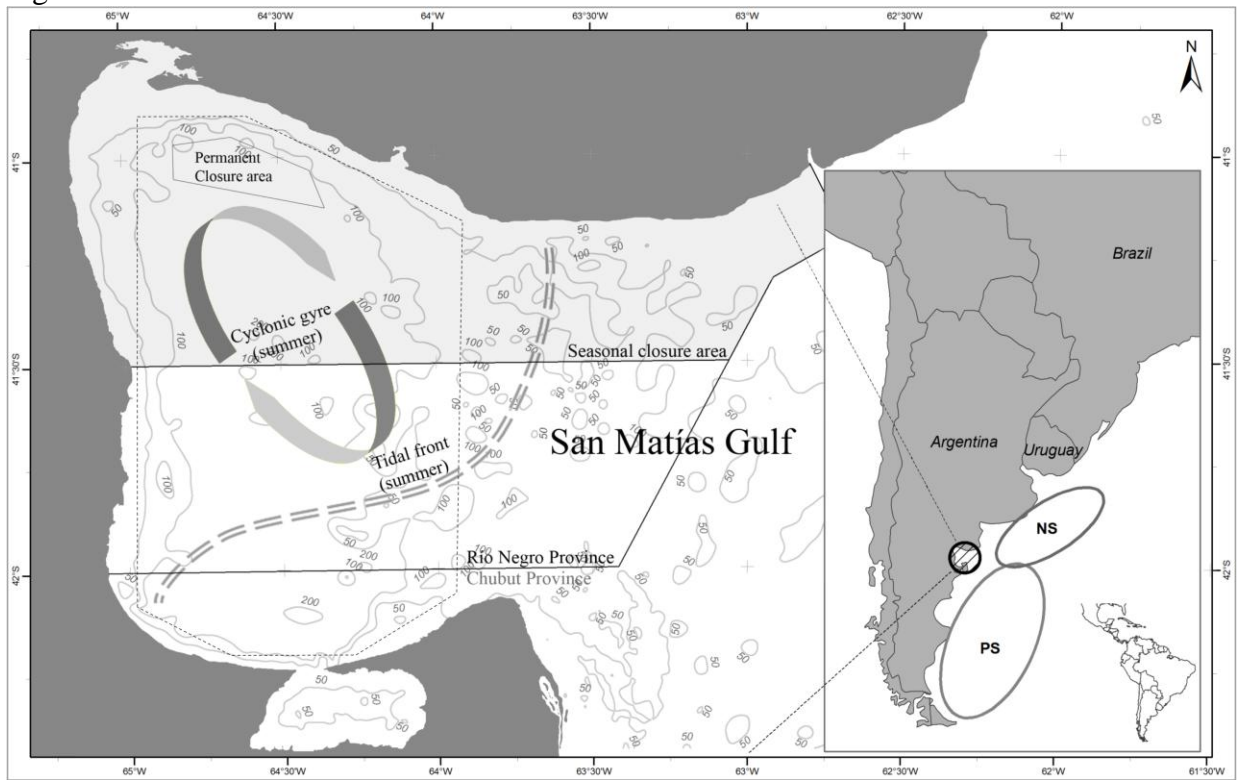
753

754 Figure 8: Hepatosomatic Index (HSI) of mature females of *Merluccius hubbsi* (>27 cm
755 of total length) in the catches of the industrial fleet. The x-axis labels indicate the month
756 of capture, the total number of individuals sampled and the number of hauls from which
757 these individuals have been obtained.

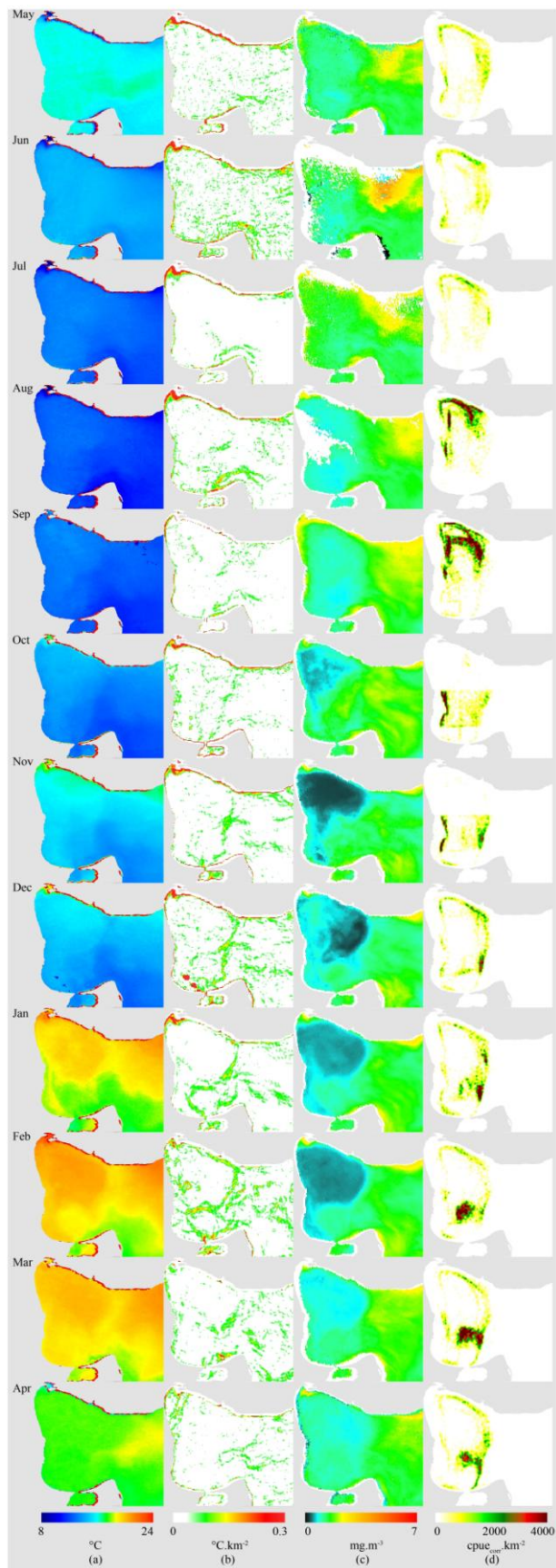
758

759 Figure 9: Colour-coded pixels by CPUEsm and Gradients. In order to illustrate each
760 season, are shown only the months of February (late spring-summer, an example of the
761 “hake season”), May (autumn, “other species season”) and September (winter- early
762 spring, “silver warehou season”). In September several pixels (purple) with a
763 combination of “High CPUEsm” and “Low Gradients” were found. In this month “High
764 Gradients” pixels were not found, in consequence, the combination (high gradients-low
765 CPUEsm) was not possible.

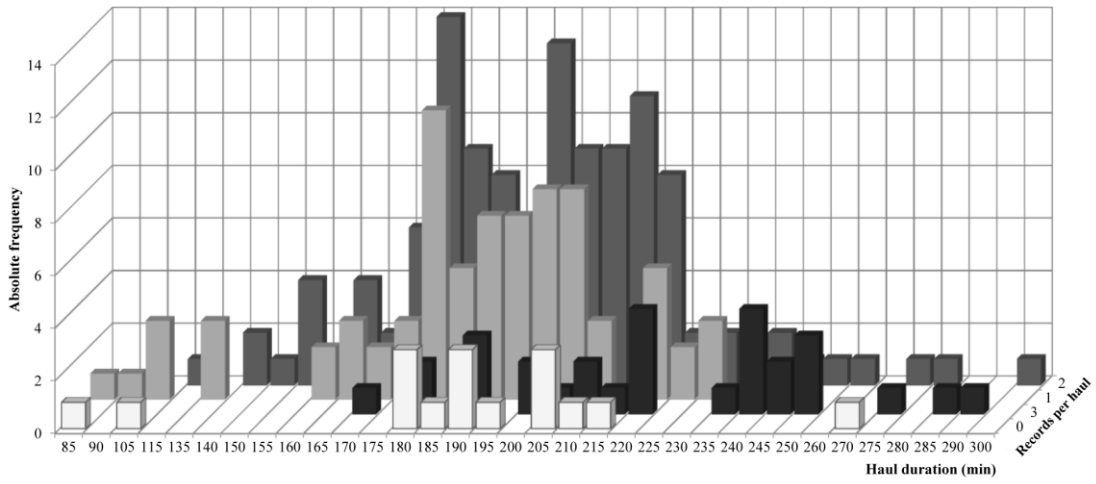
766 FIGURES
767
768 Figure 1



769
770

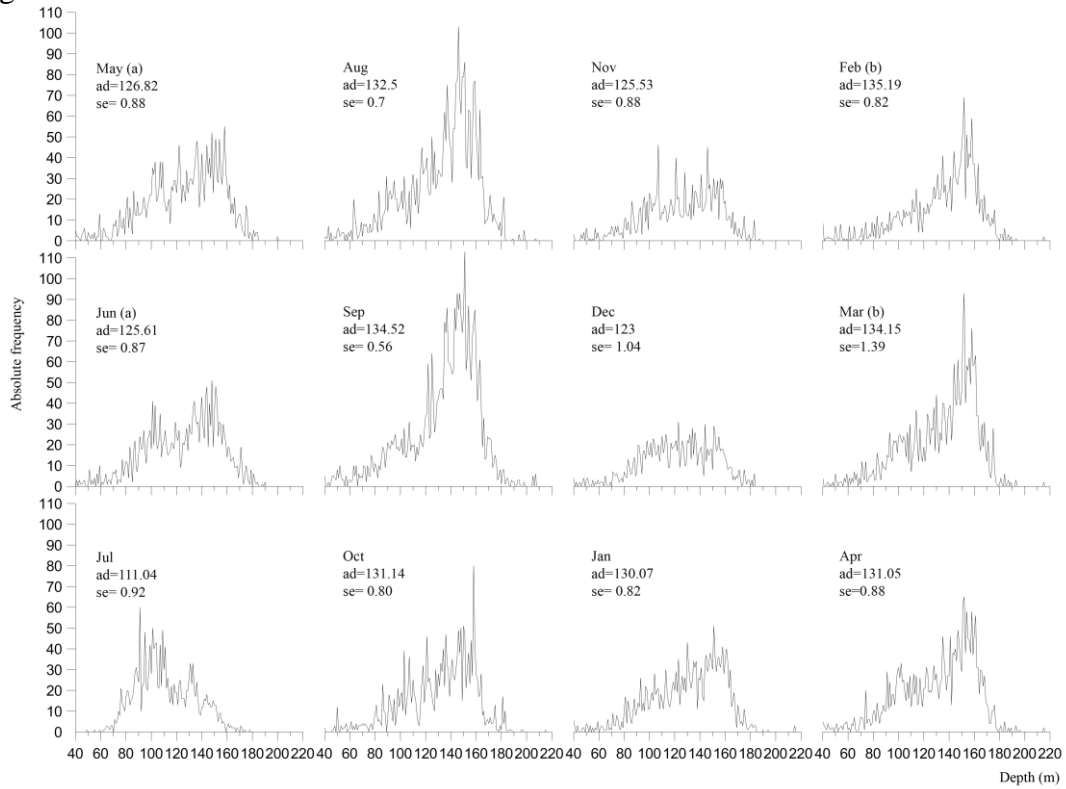


774 Figure 3



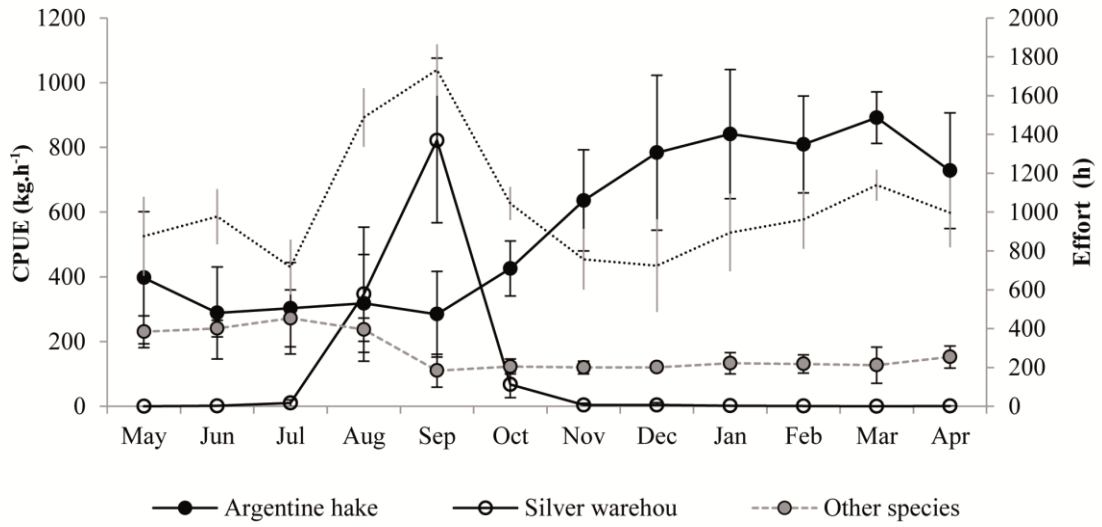
775
776
777
778
779
780
781
782
783
784
785

Figure 4



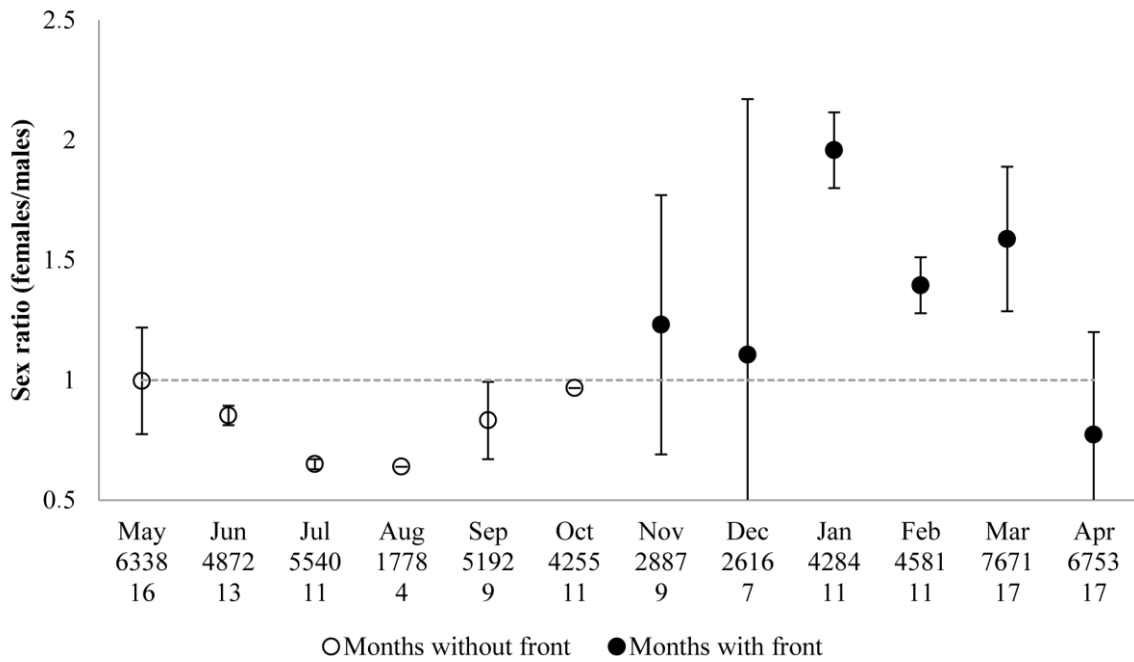
786
787

788 Figure 5



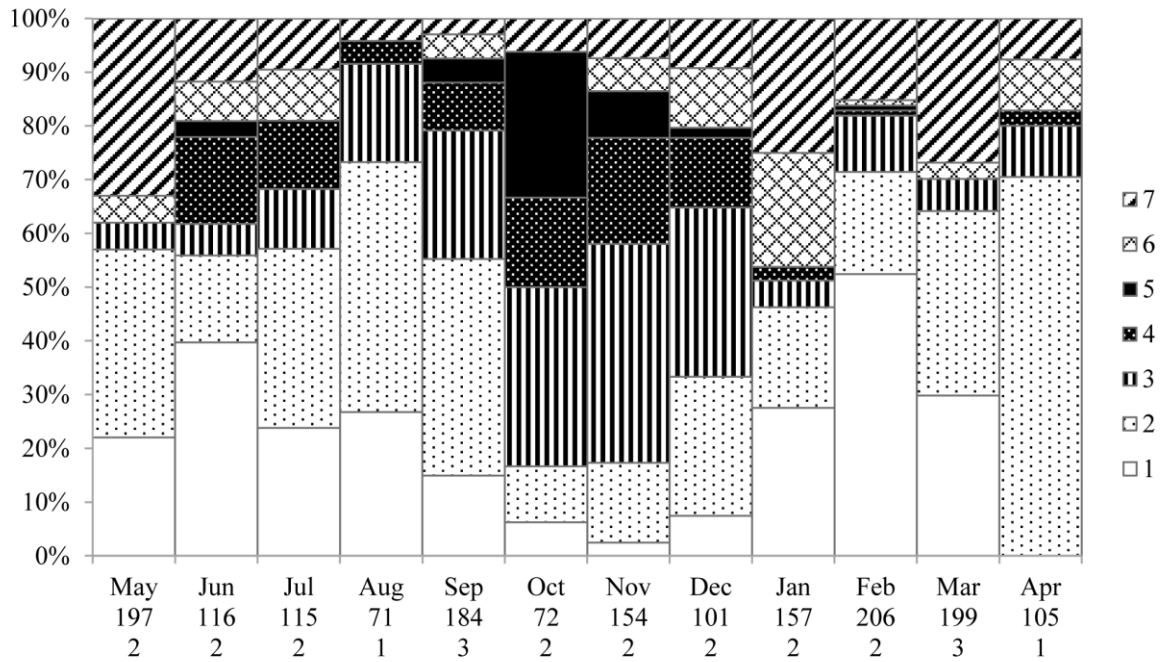
789
790
791
792
793
794
795
796
797
798
799

800 Figure 6



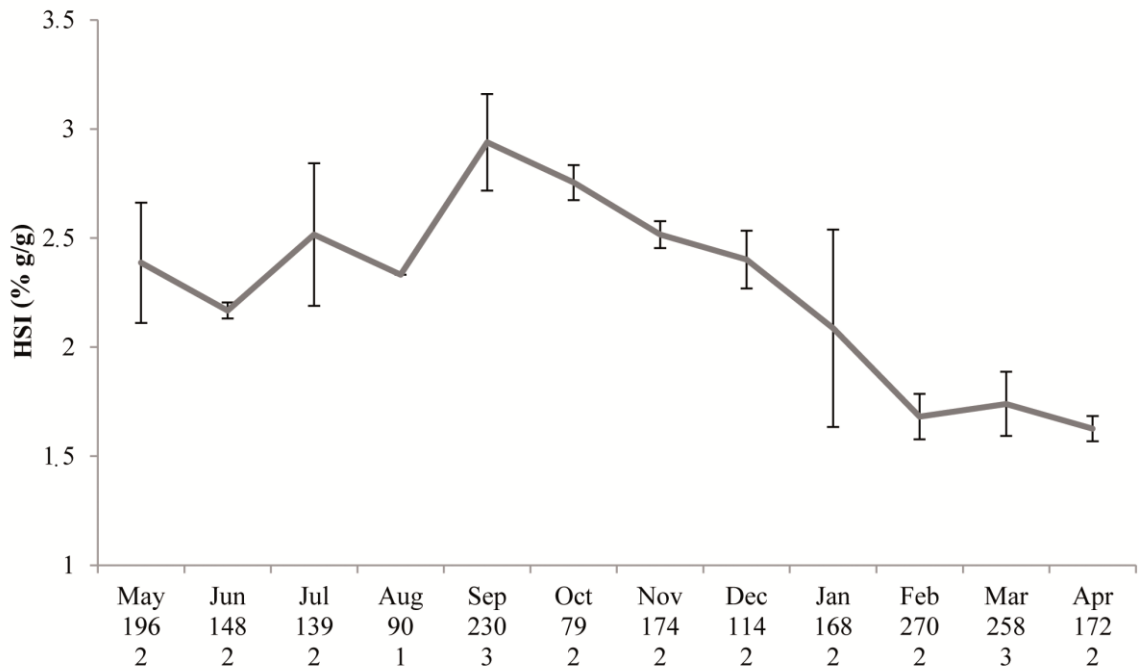
801
802

803 Figure 7



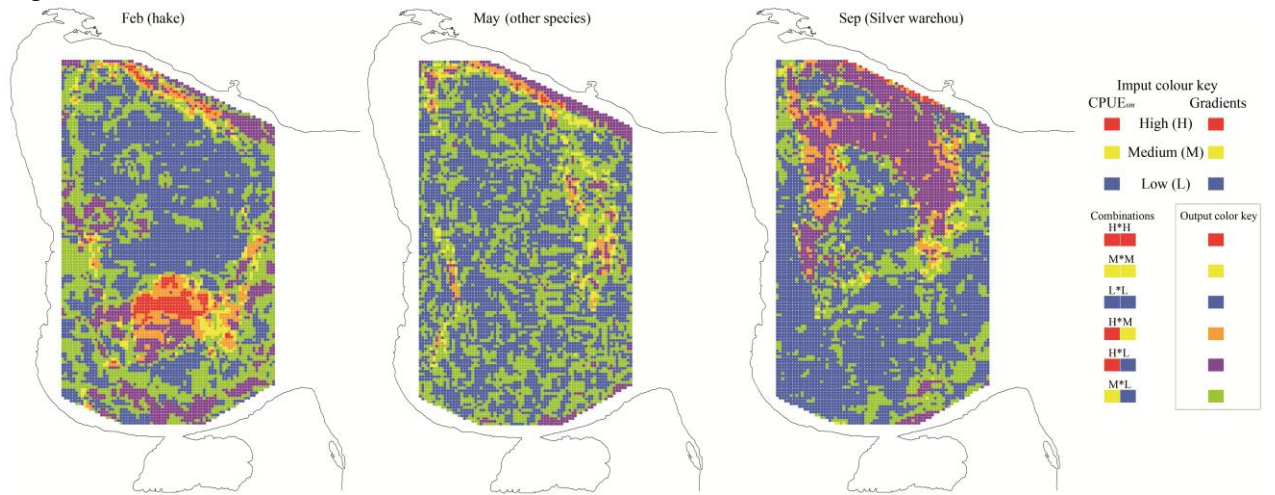
804
805
806
807
808
809
810
811
812
813

Figure 8



814
815

816 Figure 9



817